The Qualitative Analysis of Single Shot Fast Spin Echo (SSFSE) and Maximum Intensity Projection (MIP) on Magnetic Resonance Cholangiopancreatography

Cheol-Soo Park[1,2], Jae-Hwan Cho[3,4]*, Hae-Kag Lee[4], Kyung-Rae Dong[5,6], Woon-Kwan Chung[6],
Jong-Min Seok[7], Man-Seok Han[8], Sun-Yeob Lee[1], Eun-Hoe Goo[9], and Eng-Chan Kim[2]

[1]Department of Radiological Science, Hanlym College, Chuncheon 200-711, Korea
[2]Department of Physics, Yeungnam University, Daegu 705-717, Korea
[3]Department of Radiological Science, Gyeongsan University College, Gyeongsan 712-718, Korea
[4]Department of Computer Science and Engineering, Soonchunhyang University, Asan 336-745, Korea
[5]Department of Radiological Technology, Gwangju Health College University, Gwangju 506-701, Korea
[6]Department of Nuclear Engineering, Chosun University, Gwangju 501-759, Korea
[7]Department of Radiology, Nationnal Police Hospital, Seoul 138-708, Korea
[8]Department of Radiological Science, Kangwon National University, Sam Cheok 245-907, Korea
[9]Department of Diagnostic Radiology, Seoul National University Hospital, Seoul 110-744, Korea

3-dimensional magnetic resonance cholangiopancreatography (MRCP) images reconstructed using the maximum intensity projection technique were analyzed qualitatively in patients diagnosed with pancreatobiliary diseases to determine their diagnostic utility. Single shot fast spin echo (SSFSE), fast spin echo (FSE) and 3-dimensional reconstructive images were acquired from 20 patients diagnosed histologically with pancreatobiliary diseases using a 3.0T MR scanner. According to qualitative analysis, the fast spin echo images and 3-dimensional reconstructed images of the hepatic duct, gall bladder and common bile duct had a higher signal to noise ratio (SNR) than the single shot fast spin echo images. Fast spin echo images and 3-dimensional reconstructed images did not show any differences. The contrast to noise ratio of the hepatic duct, gallbladder and common bile duct on the fast spin echo images and 3-dimensional reconstructed images was higher than that of the single shot fast spin echo images. The fast spin echo images and 3-dimensional reconstructed images showed similar quality.

Keywords : MRCP, SSFSE, FSE, 3D reconstruction image, SNR, CNR

1. Introduction

Pancreatobiliary diseases are diagnosed using a range of test methods. Among them, abdominal computerized computed tomography (CT) is a simple, rapid and complication-free test. Of the many pancreatobiliary diseases, the accuracy of a diagnosis of bile duct stones differs according to the size of the bile duct stones, stone type and whether the bile duct is dilated. Moreover, the diagnosis rate for small size common bile duct stones is low [1]. Endoscopic retrograde cholangiopancreatography (ERCP) is performed on patients in whom an accurate diagnosis by such tests is difficult. Percutaneous transhepatic cholangiography (PTC) is performed on patients

who cannot undergo an ERCP test [2]. ERCP is believed to be the optimal standard test for the diagnosis and treatment of pancreatobiliary diseases, and has advantages in that its diagnosis and treatment can be carried out simultaneously. On the other hand, ERCP is dependent on the experience and expertise of the surgeons, it is invasive, and associated with complications [3].

Recently, magnetic resonance cholangiopancreatography (MRCP) has been applied frequently. This method is a good imaging technique for examining the biliary system because it is not associated with radiation exposure, is non-invasive and has high accuracy [4]. In addition, in a range of pancreatobiliary diseases, the diagnostic utility and accuracy of MRCP have been reported. Some studies suggested that MRCP can replace ERCP [5]. In regard to previous MRI images of the liver and biliary system, the image quality is low, the test takes a long time, breathing

must be held for a long time during the test, and it is difficult to acquire satisfactory images. Recently, images could be acquired within a short time with the application of a single shot fast spin echo (SSFSE) [5, 6]. On the other hand, in previous MRCP, it was difficult to assess simultaneously the presence or absence of stenosis of the pancreatobiliary system, and whether the biliary duct is dilated or not, etc.. Therefore, it is important to obtain 3-dimensional images to make an overall diagnosis. The maximum intensity projection aims to obtain 3-dimensional images using already acquired contrast enhanced images, and the spatial location of a contrast enhanced lesion could be assessed by applying 3-dimensional images.

Therefore, the authors compared qualitatively the MRCP images obtained by single shot fast echo technique and fast spin echo images with 3-dimensional images reconstructed using the maximum intensity projection method to assess the diagnostic utility of the 3-dimensional images.

2. Patients and Method

2.1. Patients

As subjects, 20 patients who showed dilation of the biliary duct and pancreatobiliary diseases were selected from patients who underwent abdominal ultrasonography from March 2010 to December 2010 for an accurate analysis (Fig. 1). Patients with chronic hepatitis, liver cirrhosis, or fatty liver in addition to bile duct dilation were excluded. The age of the patients ranged from 52 to 72 years (mean 62.8 years).

2.2. Data Acquisition

The MR images were obtained using a 1.5T MR scanner

Fig. 1. Magnetic resonance imaging of a patient showing bile duct dilation.
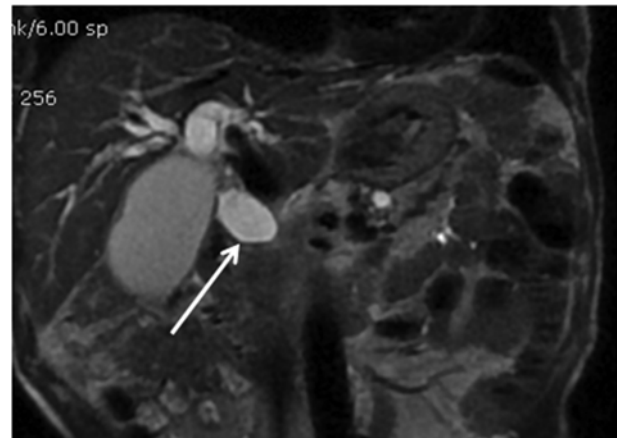
Fig. 2. Applying the single shot fast spin echo imaging technique; a T2 weighted image was obtained using the breath hold method.

(Signa 1.5T HDx. GE Healthcare. Milwaukee. WI, USA), and a HD T/R 8ch spine array coil (*In vivo* Corp. Gainesville. FL, USA) and phased array multi-coil were used. Before the study, the T2 weighted coronal images (TR: time of repetition = 2000 msec, TE: time of echo = 102 msec, NEX: average = 1) were obtained to assess the level of bile duct dilation by applying the single shot fast spin echo imaging method and breath hold techniques (Fig. 2). First, using the single shot fast spin echo imaging method, the T2 weighted coronal images were obtained by the breath hold technique using fat saturation methods. The imaging variables are as follows (Fig. 3). TR: 2400 ms, TE: 1000 ms, Matrix: 352 × 224, NEX: 1, Slice thickness: 80 mm, FOV (field of view): 340 mm, Scan Time: 59 sec. In addition, T2 weighted coronal images were obtained by applying respiratory-triggered techniques and fat saturation techniques using the fast spin echo imaging method. The imaging variables were as follows (Fig. 4). TR: 3000 ms, TE: 560 ms, Matrix: 320 × 224, NEX: 2, Slice thickness: 14 mm, FOV: 359 mm, Scan Time: 260
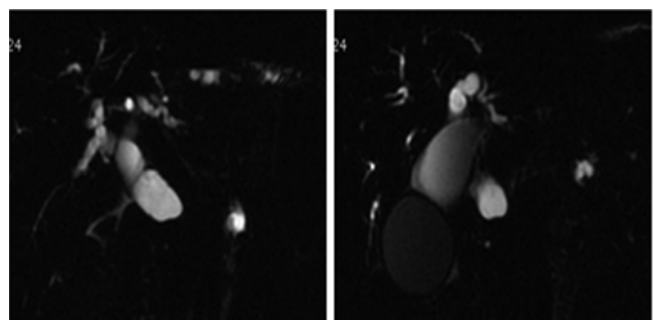
Fig. 3. Breath hold T2 weighted image of the coronal plane was obtained using the fat saturation method in SSFSE imaging.
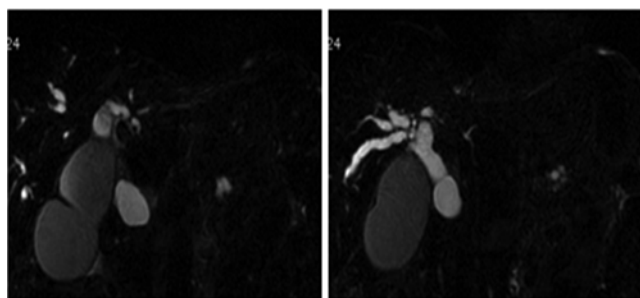
Fig. 4. T2 weighted image of the coronal plane was obtained using respiratory-triggered and fat saturation method in FSE imaging.

sec. The T2 weighted images acquired by the application of FSE techniques were sent to an Advantage Workstation (Ver. 4.3, Revision 4, GE Healthcare. Milwaukee. WI), and 3-dimensional reconstruction images were obtained using the maximum intensity projection technique. The section thickness was 100 mm, and the angle was rotated 15° in the right and left directions (Fig. 5). The signal intensity of an identical area was measured on the acquired 3 images (single shot fast spin echo image, fast echo image, and the 3-dimensional reconstructed image of fast spin echo images). The measured areas were the hepato-biliary duct area, center area of the gallbladder, and the common bile duct area; each area has three regions of interest (ROI). The size of the area of interest was 10 mm^2 (Fig. 6). As qualitative analysis methods, the signal to noise ratio in the area of interest on the three images (single shot fast echo images, fast echo image and 3-dimensional reconstruction image of the fast spin echo images) was obtained and averaged. The contrast to noise ratio (CNR) of each area of interest was obtained and averaged based on the signal to noise ratio (SNR) of the gallbladder, and the value of the three images was analyzed. The SNR was calculated by dividing the signal intensity at a part 15 mm away forward and backward from the center area of the gallbladder and mid-gallbladder, respectively, as presented in formula 1, by the signal intensity of the background standard deviation. The CNR was determined by dividing the difference between the signal intensity of the gallbladder and the other ROI by that of background standard deviation.

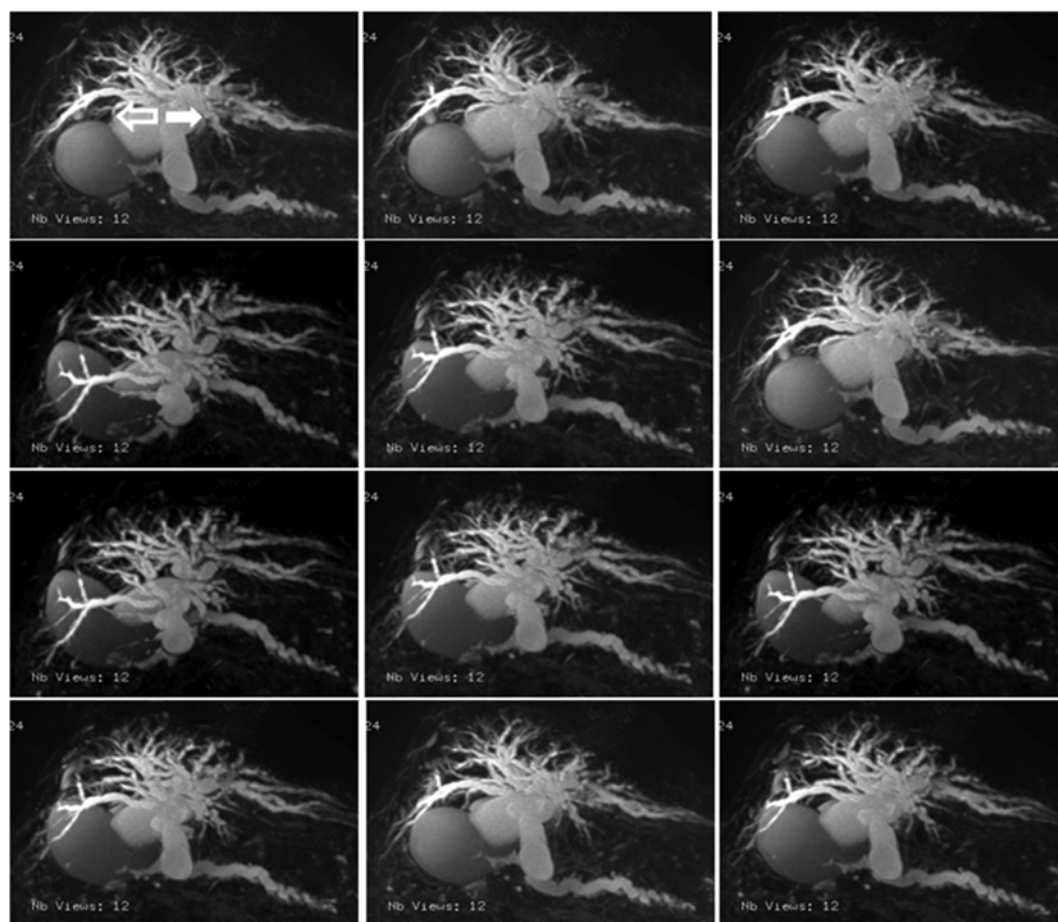The background standard deviation is presented as the

Fig. 5. Reconstruction of the 3-dimensional images by the application of the maximum intensity projection method (left right).
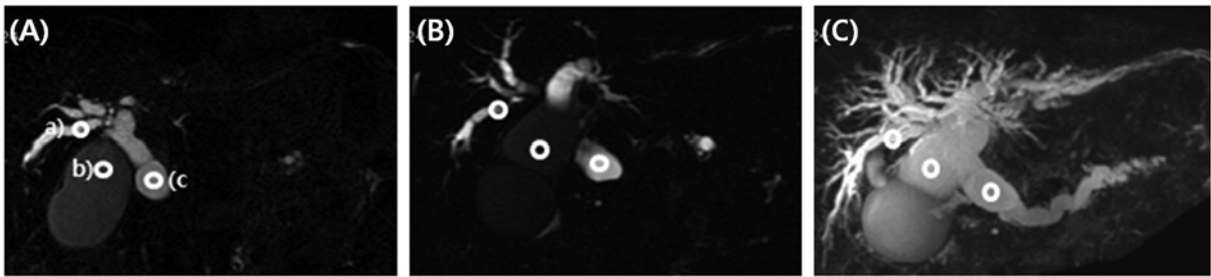
Fig. 6. Breath hold T2 weighted image using the fat saturation method in SSFSE imaging (A), T2 weighted image using respiratory-triggered and fat saturation method in FSE imaging (B) and reconstruction image of FSE image with MIP (C). The ROIs are the hepatobiliary duct area (a), center area of the gallbladder (b) and common bile duct area (c) in all of the three images.

mean and standard deviation by measuring two areas, the left upper area and right lower area of the abdominal surface, which is the phase encoding direction.

$$SNR = \frac{SI\ (region,\ surrounding\ tissues)}{SDN} \qquad (1)$$

SNR: signal to noise ratio
SDN: standard deviation of noise in the background
SI: signal intensity

$$CNR = \frac{SI\ (region) - SI\ (surrounding\ tissues)}{SDN} \qquad (2)$$

CNR: contrast to noise ratio
SDN: standard deviation of noise in the background
SI: signal intensity

The difference in the mean signal to noise ratio and the contrast to noise ratio of the area of interest acquired from the three images was analyzed using a paired t-test (paired T test SPSS win 17.0). A p-value < 0.05 was considered significant.

3. Results

Although quantitative analysis revealed that the SNR of

Table 1. Signal to noise on the SSFSE, FSE, and Reconstruction images.

Group	SNR (Mean ± SD)		
	HD	GB	CBD
SSFSE	10.24 ± 3.22	5.21 ± 0.24	12.31 ± 2.29
FSE	12.25 ± 2.29	6.24 ± 1.43	14.13 ± 0.27
p	0.035[*]	0.025[*]	0.020[*]
SSFSE	10.24 ± 3.22	5.21 ± 0.24	12.31 ± 2.29
Reconstruction image	11.77 ± 2.28	6.72 ± 2.43	13.98 ± 3.33
p	0.025[*]	0.035[*]	0.030[*]
FSE	12.25 ± 2.29	6.24 ± 1.43	14.13 ± 0.27
Reconstruction image	11.77 ± 2.28	6.72 ± 2.43	13.98 ± 3.33
p	0.070[**]	0.052[**]	0.065[**]

SNR signal to noise ratio, HD hepatic duct, GB gallbladder, CBD common bile duct, SSFSE single shot fast spin echo, FSE fast spin echo, SD standard deviation
Interaction effect using an paired T test
[*] $p < 0.05$, [**] $p > 0.05$

the SSFSE and FSE images and the three-dimensional reconstruction of the FSE image was not different in all three areas of the hepatic duct, gallbladder and common bile duct, individual analysis found that the SNR of the FSE image and its three-dimensional reconstruction image was higher than that of the SSFSE image in all three parts
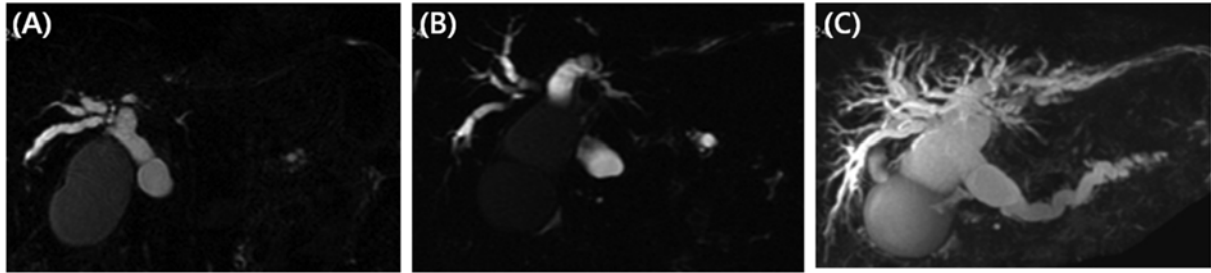

Fig. 7. Breath hold T2 weighted image using fat saturation method in SSFSE imaging (A), T2 weighted image using respiratory-triggered and fat saturation method in FSE imaging (B) and reconstruction image of FSE image with MIP (C). SNR is higher in the FSE image and reconstruction image compared to the SSFSE image and was not different between the FSE image and reconstruction image.

Table 2. Contrast to noise ratio of SSFSE, FSE, and Reconstruction images.

Group	CNR (Mean ± SD)	
	HD	CBD
SSFSE	2.18 ± 1.14	2.24 ± 1.31
FSE	3.02 ± 2.11	2.73 ± 1.31
p	0.015*	0.020*
SSFSE	2.18 ± 1.14	2.24 ± 1.31
Reconstruction image	2.98 ± 1.22	2.73 ± 1.02
p	0.035*	0.025*
FSE	3.02 ± 2.11	2.73 ± 1.31
Reconstruction image	2.98 ± 1.22	2.73 ± 1.02
p	0.060**	0.055**

CNR = contrast to noise ratio, HD = hepatic duct, CBD = common bile duct, SSFSE = single shot fast spin echo, FSE = fast spin echo, SD = standard deviation
Interaction effect using a paired T test
* $P < 0.05$, ** $P > 0.05$

(P < 0.05) but the difference between the FSE image and three-dimensional reconstruction image was not significant (P > 0.05) (Table 1) (Fig. 7).

The CNR of the SSFSE and FSE images and three-dimensional reconstruction image of the FSE image was similar but individual analysis showed that the SNR of the FSE image and its three-dimensional reconstruction image was higher than that of the SSFSE image in the three areas (P < 0.05). On the other hand, there was no significant difference between the FSE image and reconstruction image (P > 0.05) (Table 2).

As a result, the SNR and CNR of the three-dimensional reconstruction image were higher than those of the SSFSE image and were not largely different from those of the FSE image to show a similar image quality.

4. Discussion

The sensitivity and specificity of MRCP are excellent for evaluating the pancreatobiliary system, and it has been performed prior to ERCP for a diagnosis of pancreatobiliary diseases [4]. In addition, it is a non-invasive test, and provides good quality projection and cross section images of the pancreatobiliary system without an oral or intravenous injection of contrast agents, and can evaluate the lesions in areas other than the bile duct. Furthermore, its dependency on the examiner is low, and exposure to ionized radiation can be avoided [7]. Despite these advantages, the inadequate spatial resolution needed to detect small lesions is one of its shortcomings [8]. On the other hand, the following advantages have been realized with the recent development of single shot fast spin echo
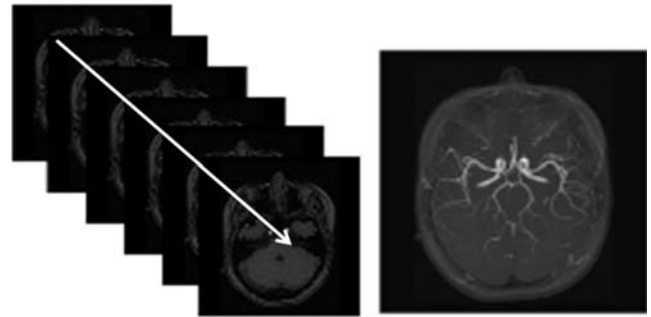

Fig. 8. Source images and reconstituted images through three-dimensional MIP.

and other fast pulse systems: images can be obtained by short breaths, the influence of artifacts generated by movement can be reduced, and the spatial resolution capacity and signal to noise ratio are increased [9]. In addition, the spatial resolution capacity has been improved further with the development of 3-dimensional fast spin echo techniques [10-13]. Kim *et al.* compared the diagnostic efficacy of single shot fast spin echo and 3-dimensional fast spin echo patients with bile duct stones [14]. The diagnostic accuracy of bile duct stones of the two techniques was similar. In the present study, the two techniques were compared and evaluated qualitatively, not quantitatively. The reconstructed images were obtained using a 3-dimensional maximum intensity projection method applying the data obtained by the fast spin echo technique and compared.

Three-dimensional MIP used in this study shows reformed images by selecting maximum intensity pixels after securing primarily source images. In other words, if a certain direction of projection is determined in total or some image, all pixels except maximum and minimum intensity ones among those parallel to the direction are deleted to present relatively high intensity pixels. It is mainly used to examine the blood vessels (Fig. 8).

According to the results, the SNR was higher in the FSE image and reconstruction image than in the SSFSE image, and SNR of the FSE image and three-dimensional reconstruction image was similar. The difference in SNR was considered to be caused by the use of different parameters. First, the FSE image was secured with a longer TR compared to the SSFSE image. TR played the role of regulating the amount of protons moving to transverse magnetization due to the RF pulse and returning to longitudinal magnetization. A longer TR led to more protons returning to longitudinal magnetization and more protons moving to transverse magnetization at the next RF pulse, resulting in an increase in the SNR. Next, FSE image was generated with a short TE. The TE was defined as the

time to reach to maximal production of echo signals after sending a RF pulse. The SNR became higher as a shorter TE produced more signals by sending a 180° RF pulse with more transverse magnetization protons remaining. In addition, FSE image were examined by raising NEX. NEX means how many times the image signals are repeated at a same site to make a single image. Generally, a higher NEX increases the SNR times. In this study, the SNR was 1.41 times higher due to the NEX being two times higher in the FSE image than in the SSFSE image. Other lateral factors of the SNR were the slice thickness and FOV, and larger pixels were generally associated with a higher SNR. The lower SNR in this study was considered to follow a relatively smaller slice thickness and FOV in the FSE image compared to the SSFSE image. On the other hand, considering various parameters, the SNR of the FSE image was increased more than that of the SSFSE image. The lack of a difference between the FSE image and its three-dimensional reconstruction image was attributed to the use of the same parameters to have no effect on the SNR. The CNR of the FSE image and its three-dimensional reconstruction image was higher than that of the SSFSE image, and the CNR of the FSE image and its reconstruction image was similar. This was attributed to the higher SNR in the FSE image and three-dimensional reconstruction image because the parameters mentioned above increased the CNR. The contrast to noise ratio of the fast spin echo images was similar to that of the 3-dimensional reconstructed images, which appears to support the results reported by Kim *et al.* [14]. Nevertheless, it was difficult to assess the entire fast spin echo image simultaneously. Moreover, the images reconstructed by the application of a 3-dimensional maximum intensity projection method allowed an assessment of the spatial location, which can extend the diagnostic range. In other words, the 3-dimensional reconstructed images increased the spatial efficacy without changing the signal intensity. In this study, the signal to noise ratio of the fast spin echo images was higher than that of the single shot fast spin echo images.

This study had several limitations. First, it was difficult to assign an area of interest because of the difference between the 2-dimensional images fast spin images and reconstructed 3-dimensional images. Second, identical parameters were not used in the single shot fast spin echo images and fast spin images, making it difficult to obtain objective research results. Nevertheless, the assignment of identical parameters causes substantial difficulties because they use different pulse types. Third, the signal intensity was different depending on the patients' characteristics. Therefore, it was not measured under identical conditions.

Fourth, the number of patients was too low to make a definitive conclusion. Therefore, further study with a larger cohort will be needed.

5. Conclusions

The SNR of the three-dimensional reconstructed FSE image was higher than that of the SSFSE images in three areas of the hepatic duct, gallbladder and common bile duct, and the CNR was also higher than that of the SSFSE. The difference in the CNR between the FSE image and three-dimensional reconstruction image was not significant. Overall, three-dimensional images using MIP in magnetic resonance cholangio pancreatography (MRCP) provides better information on the location with higher signal intensity than SSFSE and FSE images, and will be more helpful for diagnosis.

In MRCP, the 3-dimensional images produced using the maximum intensity projection method provide more information on the location than fast spin echo images and create images with high signal intensity, thereby providing superior information for diagnosis.

References

[1] J. K. Lee, P. L. Rhee, J. H. Lee, K. T. Lee, S. H. Choi, J. H. Noh, J. J. Kim, K. C. Ko, S. W. Paik, and J. C. Rhee, Korean J. Gastroenterol. **29**, 85 (1997).
[2] R. K. Yadar, S. Magu, A. Sharma, J. Sen, P. Malik, and J. Arora, J. Indian Med. Assoc. **96**, 330 (1998).
[3] M. K. Bilbao, C. T. Dotter, T. G. Lee, and R. M. Katon, Gastroenterology **70**, 314 (1976).
[4] B. K. Wallner, K. A. Schumacher, W. Weidenmer, and J. M. Friedrich, Radiology **181**, 805 (1991).
[5] R. E. Hintze, A. Adler, W. Veltzke, H. Abou-Rebyeh, R. Hammersting, T. Vog, and R. Felix, Endoscopy **29**, 182 (1997).
[6] N. Holzknecht, J. Gauger, M. Sackmann, R. F. Thoeni, J. Schurig, J. Holl, M. Weinzierl, T. Helmberger, G. Paumgartner, and M. Reiser, Radiology **206**, 657 (1998).
[7] F. V. Coakley, and L. H. Schwartz, J. Magn. Reson. Imaging **9**, 157 (1999).
[8] C. Aube, B. Delorme, T. Yzet, P. Burtin, J. Lebigot, P. Pessaux, C. Gondry-Jouet, J. Boyer, and C. Caron, Am. J. Roentnol. **184**, 55 (2005).
[9] E. J. Yun, C. S. Choi, D. Y. Yoon, Y. C. Yoon, S. J. Park, Y. L. Seo, J. H. Moon, and K. J. Lim, J. Korean Radiol. Soc. **49**, 483 (2003).
[10] A. S. Fulcher, M. A. Turner, G. W. Capps, A. M. Zfass, and K. M. Baker, Radiology **207**, 21 (1998).
[11] E. C. Kaltenthaler, S. J. Walters, J. Chilcott, A. Blakeborough, Y. B. Vergel, and S. Thomas, BMC Med. Imaging **6**, 9 (2006).

[12] T. J. Vogl, W. O. Schwarz, M. Heller, C. Herzog, S. Zangos, R. E. Hintze, P. Neuhaus, and R. M. Hammersting, Eur. Radiol **16**, 2317 (2006).

[13] J. A. Soto, M. A. Barish, O. Alvarez, and S. Medina, Radiology **215**, 737 (2000).

[14] J. A. Kim, E. J. Yun, C. S. Choi, D. Y. Yoon, S. J. Park, Y. L. Seo, Y. J. Lee, and J. H. Moon, J. Korean Radiol. Soc. **54**, 97 (2006).